ACS Biomaterials SCIENCE & ENGINEERING

pubs.acs.org/journal/abseba Article

Potential of an Aligned Porous Hydrogel Scaffold Combined with Periodontal Ligament Stem Cells or Gingival Mesenchymal Stem Cells to Promote Tissue Regeneration in Rat Periodontal Defects

Wenhao Wang, Ao Wang, Gaofu Hu, Mengyao Bian, Lili Chen, Qian Zhao, Weilian Sun, and Yanmin Wu*

Cite This: https://doi.org/10.1021/acsbiomaterials.2c01440 Read Online

ABSTRACT: Periodontal tissue regeneration is a major challenge in tissue engineering due to its regenerated environment complexity. It aims to regenerate not only the supporting alveolar bone and cementum around teeth but also the key connecting periodontal ligament. Herein, a constructed aligned porous hydrogel scaffold carrying cells based on chitosan (CHI) and oxidized chondroitin sulfate (OCS) treated with a freeze-casting technique was fabricated, which aimed to induce the arrangement of periodontal tissue regeneration. The microscopic morphology and physical and chemical properties of the hydrogel scaffold were evaluated. The biocompatibilities with periodontal ligament stem cells (PDLSCs) or gingival-derived mesenchymal stem cells (GMSCs) were verified, respectively, by Live/Dead staining and CCK8 in vitro. Furthermore, the regeneration effect of the aligned porous hydrogel scaffold combined with PDLSCs and GMSCs was evaluated in vivo. The biocompatibility experiments showed no statistical significance between the hydrogel culture group and blank control ($P > 0.05$). In a rat periodontal defect model, PDLSC and GMSC hydrogel experimental groups showed more pronounced bone tissue repair than the blank control ($P < 0.05$) in micro-CT. In addition, there was more tissue repair ($P < 0.05$) of PDLSC and GMSC hydrogel groups from histological staining images. Higher expressions of OPN, Runx-2, and COL-I were detected in both of the above groups via immunohistochemistry staining. More importantly, the group with the aligned porous hydrogel induced more order periodontal ligament formation than that with the ordinary hydrogel in Masson's trichrome analysis. Collectively, it is expected to promote periodontal tissue regeneration utilizing an aligned porous hydrogel scaffold combined with PDLSCs and GMSCs (CHI−OCS−PDLSC/GMSC composite), which provides an alternative possibility for clinical application.

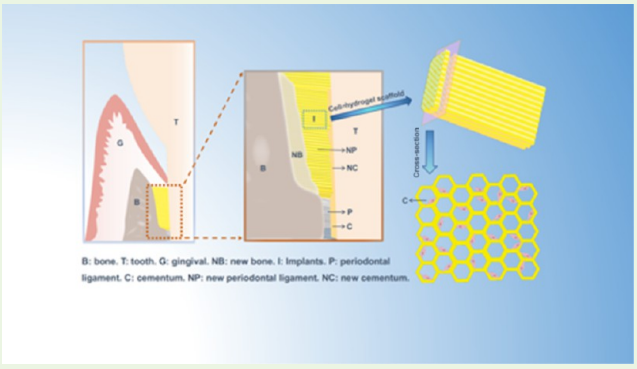

KEYWORDS: *periodontitis, tissue regeneration, stem cells, aligned porous hydrogel, freeze-casting*

1. INTRODUCTION

Periodontitis is a type of chronic inflammatory disease initiated by a dental plaque biofilm combined with local stimulatory and systemic factors. Due to bacterial invasion and autoimmune reactions, it can gradually destroy the periodontal supporting tissue, which eventually leads to tooth loosening and loss.[1] However, the existing treatments for advanced periodontal disease only control the infection and delay the progression of periodontal disease. There is no effective method to regenerate the lost periodontal tissue completely.

Hydrogels are often used as stem cell scaffold materials for various tissue engineering including periodontal regeneration.[2] In recent years, various new hydrogel materials have been designed to achieve the goal of periodontal tissue regeneration, such as fiber-reinforced hydrogel,[3] heat-sensitive chitosan (CHI) hydrogel,[4] high-stiffness transglutaminase crosslinked hydrogel,[5] etc. These have been proven to possess promoting effects on periodontal regeneration. However, native periodontal ligament fibers are vertically inserted into the cementum and connected with the alveolar bone in a regular way, withstanding cushion and chewing force. To reconstruct the structure and function of periodontal tissue, it is necessary to achieve both soft and hard tissue regeneration.[6] For this purpose, a multilayer nanocomposite hydrogel scaffold has been designed. As an alternative regeneration method, it has achieved a good repair effect.[7] However, the preparation process complexity and structure of its multilayer is difficult to adapt

Received: December 3, 2022
Accepted: March 13, 2023

to different clinical periodontal defect shapes. Therefore, it is our goal to design an economical, convenient, and promising hydrogel material.

CHI as a biomaterial has been fully studied in stomatology for processes, such as bone regeneration, periodontal regeneration, and so on. Extracted from chitin, CHI has good biocompatibility, non-toxicity, degradability, and good antibacterial properties.[8−12] Chondroitin sulfate (CS) is a glycosaminoglycan composed of glucuronic acid and acetylgalactosamine, which plays an important role in regulating inflammation, intracellular signal transduction, formation of an extracellular matrix, cell surface protein connection, and the cartilage phenotype. CS has been reported to promote the maturation of osteoblasts and calcification of bone tissue by interacting with transforming growth factors. It also promoted the growth, proliferation, and adhesion of osteoblasts by inducing the adsorption of calcium ions, improving the bone morphogenetic protein (BMP)-carrying system, and increasing the local BMP concentration, which facilitated the formation of the new bone.[13−15] Oxidized chondroitin sulfate (OCS) contains aldehyde groups that are expected to react with CHI amino groups by the Schiff base, which does not change its physiological characteristics.[16−18] Based on the above research background, we chose CHI and OCS as the two substrates of the hydrogel.

Mesenchymal stem cells (MSCs) are a group of stem cells with self-renewal, multidifferentiation, and immune regulation capabilities in the host. Human periodontal ligament stem cells (PDLSCs) are the adequately studied target cells for periodontal regeneration at present.[19] They have the potential to differentiate into fiber, fat, and bone in multiple directions. The proliferation potential of PDLSCs was stronger than that of bone marrow mesenchymal stem cells (BMMSCs) and dental pulp stem cells (DPSCs).[20] Gingival-derived mesenchymal stem cells (GMSCs) are newly discovered MSCs derived from gingival tissue in recent years.[21] Gingival tissue can be easily obtained through minimally invasive surgery, which means that this kind of cell is relatively richer in resources than PDLSCs.[22−24] Previous studies showed both GMSCs and PDLSCs possessed the capacity to generate new fiber and bone following ectopic transplantation. Human PDLSCs exhibited a more effective differentiation potential than GMSCs, irrespective of incubation conditions.[25] Various reports have indicated bidirectional interactions between MSCs and inflammatory cells or molecules. For example, inflammatory cells can recruit MSCs and direct their migration and differentiation to exert anabolic effects on bone repair.[26] The multidirectional differentiation ability of two kinds of cells might decrease under the inflammation condition. However, compared with PDLSCs, GMSCs showed less inflammation-related changes like decreased osteogenic potential both in vitro and in vivo under inflammatory conditions.[25] In addition, many studies have proved that the GMSC has superior immune regulation in inflammatory environments.[27−31] For example, GMSC-derived exosomes can reduce the release and expression of inflammatory factors in a high-fat microenvironment, inhibit the M1 macrophage phenotype, regulate inflammatory immune cells through the interleukin 10 signal, and alleviate inflammatory bowel disease. Therefore, GMSCs and PDLSCs may be promising candidates for periodontal regeneration engineering. In this study, we will compare the regeneration and differentiation abilities of GMSCs and PDLSCs in vivo and in vitro and verify the periodontal regeneration potential of delivering cells with hydrogel scaffold materials directly to the periodontal defect.

To carry stem cells, the porous diameter of cells carrying hydrogels is expected to be larger than the cell diameter. However, the porous structure of most cells carrying hydrogels is uneven and disordered, which is not conducive to the nutrition and gas exchange necessary for cell proliferation and differentiation. Hopefully, the construction of cells carrying hydrogels with a uniform size and aspecific directional aperture may be the key for transplant materials and periodontal complexes (Figure 2). In our previous research, enzyme-degrading hydrogels with directional pore size through freeze-casting and condensation gelation by the mixed solution of CHI and oxidized dextran have been prepared. In the swelling state of the hydrogel, we got the microtubule pores arranged along the freezing direction. The pore size could be adjusted within 20−100 μm through controlling the temperature in the freeze-casting procedure.[32] Other researchers have synthesized regularly arranged type I collagen fiber materials,[33] freeze-cast chitosan alginate hydrogel biomaterials,[34] etc. through freeze-casting technology, which provides new directions for biomedical applications such as muscle and nerve regeneration.

In this study, CHI and OCS were used to construct a porous hydrogel by the Schiff base reaction with uniform size and direction by the freeze-casting technique. The micro-morphology, physical and chemical properties, structural stability, and mechanical strength of the hydrogel were studied. The hydrogel delivered PDLSCs and GMSCs, two kinds of MSCs derived from the periodontal ligament and gingival tissue, respectively, to the periodontal defect area to repair it. Sprague Dawley rat (SD rat) periodontal defect models were used to evaluate the safety and effectiveness of the CHI−OCS−PDLSC/GMSC composite in inducing periodontal tissue regeneration.

2. METHODS AND MATERIALS

2.1. Isolation of Cells from Human Gingiva and Periodontal Ligament. Approved by the Ethics Committee of the Second Affiliated Hospital of Zhejiang University (no. 2021-0647) and with informed consent from patients, extracted healthy premolars due to orthodontic treatment in patients aged 17−30 were obtained. Freshly extracted premolars were rinsed 3−5 times with phosphate buffered saline (PBS, Gibco, USA). The periodontal ligament tissue was scraped from 1/3 of the tooth root for the separation of primary periodontal ligament cells (PDL cells). The gingival tissue of the tooth neck was collected for the separation of primary gingival cells (G-cells). Periodontal ligament tissue was digested with 0.2% collagenase type II (Sigma, USA) for 30 min in a 37 °C water bath. Gingival tissue was digested with 0.2% collagenase type I (Sigma, USA). The digested tissues were then seeded in 100 mm dishes containing 15% fetal bovine serum (FBS; Gibco, USA), 100 U/mL streptomycin and penicillin (Invitrogen, USA), and Dulbecco's modified Eagle medium (DMEM, Cienry, China) and incubated at 37 °C in 5% CO_2 with the medium changed periodically every 3 days until primary cells crawled out.

2.2. Isolation of PDLSCs and GMSCs. PDLSCs and GMSCs were isolated from primary human periodontal ligament cells and primary gingival fibroblasts using Stro-1 immunomagnetic beads. Cells were counted first, and the number should not exceed 1×10^7. 50 μL of Stro-1 Antibody PE (Santa, USA) and 25 μL of m-IgG k BP-PE (Santa, USA) were added to cells for 15 min at 4 °C without light. After removing the supernatant, cells were incubated in 20 μL of FCR Blocking Reagent (Miltenyi Biotec, USA) and 20 μL of Anti-PE Microbeads (Miltenyi Biotec, USA) for 15 min at 4 °C protected from light. Cell suspension was then passed through a 70 μm cell strainer to remove large debris. With the MACS Sorting column (Miltenyi Biotec, USA) pre-wetted and Mini MAC Separation (Miltenyi Biotec, USA) installed, the cell suspension was added, and the liquid that falls

https://doi.org/10.1021/acsbiomaterials.2c01440
ACS Biomater. Sci. Eng. XXXX, XXX, XXX−XXX

naturally was collected. The negatively selected cells were rinsed 3 times with 2 mL of buffer while keeping the gray part moist during the process. After the column was removed from the device, 2 mL of buffer was added slowly with a needle cylinder 2-3 times. With the supernatant removed after centrifugation, cells collected were seeded in 100 mm cell culture dishes.

2.3. Cell Counting Kit-8 Assay. The cell proliferation curves of PDLSCs and GMSCs and the cytotoxicity of the CHI−OCS hydrogel were examined by a CCK8 assay (Apexbio, America) as follows. PDLSCs or GMSCs were seeded in 96-well plates at a density of 2×10^3 cells/well. Cell proliferation was tested at 1, 3, 5, 7, 9, 11, 13, and 15 days. Then, 10 μL of the CCK8 reagent and 100 μL of DMEM containing 10% (v/v) FBS and 1% (v/v) penicillin−streptomycin (Invitrogen, USA) were added to each well and incubated at 37 °C and 5% CO_2 for 1 h. The optical density (OD) at 450 nm was measured through a microplate reader (PerKinelmer, England).

Lyophilized samples of the hydrogel with the concentration ratio of 2:1 between CHI and OCS were cut into thin sections with a diameter of 6 mm. The samples were placed on the bottom 96-well plates after sterilization under UV light for 30 min. The groups with no materials were set as control groups (PDLSC group and GMSC group). Single-cell suspensions of 2×10^3 PDLSCs or GMSCs in 100 μL of DMEM were added to each well of a 96-well plate. To simulate the naturally degraded state of material, cells were cultured in a 37 °C, 5% CO_2 incubator. With all samples treated by following the above CCK8 method, the ODs of the two control groups, the PDLSC-HY (hydrogel combined with PDLSC) group, and the GMSC-HY (hydrogel combined with GMSC) group were read at 450 nm as described above at 1, 3, 5, 7, and 14 days.

2.4. Flow Cytometric Identification. Flow cytometry was used to identify PDLSC and GMSC surface markers. Single-cell suspensions (1×10^6 cells/mL) of two types cells were incubated with fluorescein isothiocyanate (FITC) or phycoerythrin (PE) conjugated antibodies against human CD146, CD105, CD45 (BD, USA), and Stro-1 (Santa, USA) in the dark for 30 min at 4 °C, respectively. The two types of cells were washed twice with PBS containing 2% FBS and analyzed by flow cytometry using the CytoFLEX LX (Beckman Coulter, USA).

2.5. Multiple Differentiation Potential and ALP Staining. PDLSCs and GMSCs were seeded in 6-well plates at a density of 2×10^4 cells/well and incubated with osteogenic induction medium (DMEM containing 10% FBS [Sciencell, USA], 50 μM ascorbic acid [Solarbio, China], 10 nM dexamethasone [Solarbio, China], and 10 mM sodium β-glycerophosphate [Solarbio, China]) for 21 days to confirm pluripotent differentiation potential. A 4% paraformaldehyde (PFA) (Solarbio, China) solution was used to fix the cells, and a 0.1% Alizarin Red S-Tris−HCl (Darui, China) solution was used to stain them for 30 min, followed by deionized water washing for three times. Finally, osteogenic differentiation was confirmed under the light microscope. At the same time, PDLSCs and GMSCs were seeded in 6-well plates at a density of 1×10^5 cells/well and cultured for 21 days in an adipogenic medium (DMEM containing 10% FBS, 10 μg/mL insulin [Macklin, China], 100 μM indomethacin [Macklin, China], 0.5 mM 3-isobutyl-1-methylxanthine [Macklin, China], and 1 nM dexamethasone). A 4% PFA solution was used to fix the cells for 30 min, and then, Oil Red O was used to stain them for 30 min in the dark, followed by washing with deionized water three times. Adipogenic differentiation was observed under the light microscope.

Meanwhile, PDLSCs and GMSCs were seeded in 6-well culture plates at a density of 2×10^4 cells/well and cultured with osteogenic induction medium for 14 days. The cells were fixed in 4% PFA for 30 min, treated with BCIP (Solarbio, China), and stained with an NBT alkaline phosphatase chromogenic kit (Solarbio, China) for 30 min. Then, the ALP results were observed under a light microscope after deionized water washing.

2.6. Oxidization of Chondroitin Sulfate by Sodium Periodate. OCS was synthesized following the reported procedure.[35] CS (5 g, Aladdin, China) was dissolved by stirring in deionized water (100 mL). A certain amount of $NaIO_4$ (1.2, 2.3 g, Sigma-Aldrich, USA) was added after the CS was completely dissolved. Different samples were reacted under room temperature and dark conditions for 2 and 4 h (Table 1).

Table 1. Oxidization Conditions and Different Oxidization Degrees of CS

samples	Cs (*g*)	sodium periodate (*g*)	oxidization time (*h*)	oxidization degree (mol %)
cs-1	5	1.2	2	9.3
cs-2	5	2.3	2	14.7
cs-3	5	2.3	4	20.2

After the reaction, 100 mL of absolute ethanol was added and stirred for 15 min. After precipitation at 4 °C for 6 h, the supernatant was removed, and the precipitated OCS was collected. OCS was transferred to a dialyzed bag with a cutoff at Mw = 3500 and dialyzed against deionized water at 4 °C for 7 days. The OCS solution was freeze-dried and stored at 4 °C for later use.

2.7. 2,4-Dinitrophenylhydrazine Titration. The aldehyde group content in the oxidative CS chain was quantitatively analyzed by titrating the aldehyde group with 2,4-dinitrophenylhydrazine (DNPH). CS (5 mg) of different degrees of oxidation (calculated by the molar ratio of OCS repeating units to total repeating units) was mixed with 2 M hydrochloric acid (1 mL) and 0.05 M DNPH acetonitrile (1 mL) solutions. The mixture was stirred for 1 h with magnetic stirring. After the orange precipitate formed, the solution was extracted with ethyl acetate (3 mL). The amount of unreacted DNPH was calculated based on the OD at 450 nm.

2.8. Fourier Transform Infrared Spectra. The Fourier transform infrared (FTIR) spectra were recorded in KBr pellets with a Nicolet iS50 FTIR spectrometer (Thermo Scientific Co., Waltham, MA) at 25 °C. About 2 mg volumes of CHI, CS, OCS, and CHI−OCS gel powder samples were mixed, respectively, with 100 mg of potassium bromide powder to prepare pellets for studies. The FTIR scans were recorded between 4000 and 400 cm^{-1}.

2.9. Preparation of the Aligned Porous CHI−OCS Hydrogel. Medium-viscosity CHI (Aladdin, China) was dissolved in acetic acid (2 vol %) to obtain CHI solution (2 wt %). An amount of OCS was dissolved in deionized water until the weight ratio of CHI to OCS (with the oxidation degree of 20%) was 4:1, 2:1, 1:1, or 1:2. The two solutions were stirred rapidly after being cooled down to 0 °C. The mixture solution was frozen through the freeze-casting step that has been reported in previous literature studies.[35] Briefly, the mixture solution in the fluid state was decanted into a polypropylene tube (22 mm diameter × 50 mm height), the bottom of which was close to the surface of liquid nitrogen (−196 °C), while the rest was kept at room temperature. The mixture solution was moved into a −8 °C freezer immediately after it was frozen completely. The reaction of OCS and CHI was carried out at this low temperature for 3 days. After the reaction, the resulting product was soaked in excess deionized water at 25 °C for 48 h, with water being replaced every 6 h to remove the unreacted materials. Besides, the gel synthesized by CHI and OCS with the traditional way at room temperature instead of the freeze-casting technique was used as a control.

2.10. Scanning Electron Microscopy. The micro-morphology of the CHI−OCS hydrogel synthesized with the traditional way or the freeze-casting technique was characterized with scanning electron microscopy (SEM). All samples were first lyophilized and then gold plated with a MC1000 lon sputtering coater (Hitachi, Japan). An SU8010 SEM (Hitachi, Tokyo, Japan) was used to observe the morphology at 3 kV accelerating voltage. Five hydrogel samples from each of the two hydrogels were selected for pore size analysis. 100 pores were selected randomly, and the pore size was calculated by ImageJ software (National Institutes of Health, USA). The measurement of the pore diameter is shown in the Supporting Information (Table S3).

2.11. Rheological Properties. The rheological properties of the CHI−OCS hydrogel were measured with a rotational rheometer (MCR302, Anton Paar, Austria). The hydrogel was carefully placed on the instrument table. The storage modulus (G') and loss modulus (G'') of the hydrogel were measured from 10 to 40 °C at a constant heating rate (2 °C/min) and a constant frequency (1 Hz).

https://doi.org/10.1021/acsbiomaterials.2c01440
ACS Biomater. Sci. Eng. XXXX, XXX, XXX−XXX

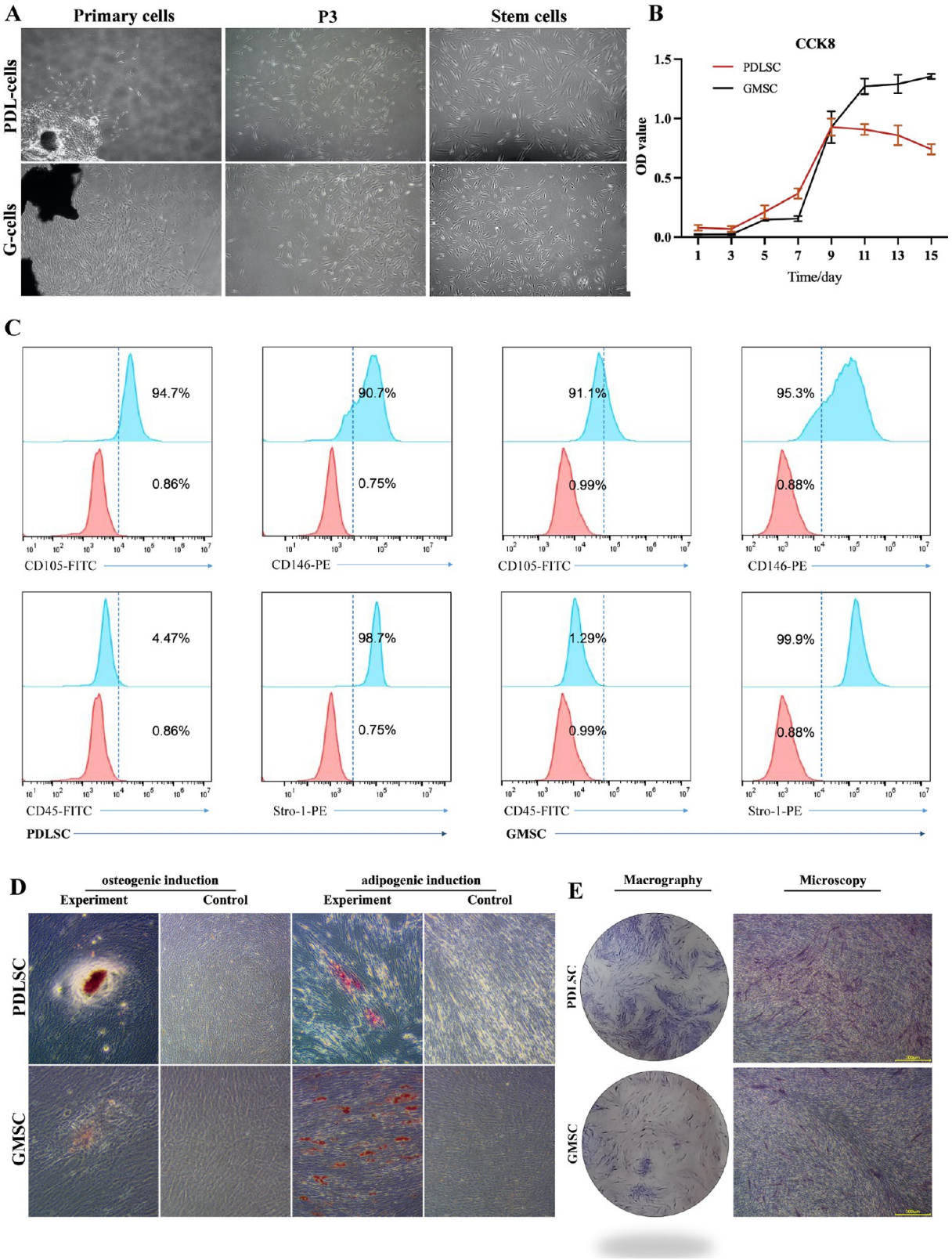

Figure 1. Culture and identification of PDLSCs and GMSCs. (A) Primary cells derived from gingiva (G-cells) and periodontal ligament (PDL-cells) and the third generation of cells (P3); the cells are spindle-like after immunomagnetic bead sorting. (B) CCK8 cell proliferation assay of PDLSCs and GMSCs. (C) Flow cytometry analysis of PDLSCs and GMSCs. (D) Multidirectional differentiation assays: osteogenic and adipogenic induction results of PDLSCs and GMSCs. (E) ALP staining: macrography and microscopy of PDLSCs and GMSCs.

2.12. Swelling Properties. CHI−OCS hydrogel samples with a concentration of 20 mg/mL at the time of preparation were used to evaluate the equilibrated swelling ratio (ESR). In short, 20 mg (W_d) samples of dried CHI−OCS hydrogel with different concentration ratios (CHI/OCS = 1:2, 1:1, 2:1, and 4:1) were immersed into 40 mL of PBS (pH = 7.4) and cultured at 37 °C. Then, the CHI−OCS

https://doi.org/10.1021/acsbiomaterials.2c01440
ACS Biomater. Sci. Eng. XXXX, XXX, XXX−XXX

hydrogels were weighed again (W_s) at various times after soaking until reaching the equilibrium state. All measurements were made using at least 3 replicates. The standard deviation for different data points is shown in the Supporting Information (Table S1). The ESR of CHI−OCS hydrogels was calculated according to the following formula

$$\text{Equilibrated swelling ratio (\%)} = (W_s - W_d)/W_d \times 100\%$$

2.13. Degradation In Vitro. CHI−OCS hydrogel samples with a concentration of 20 mg/mL at the time of preparation were used to analyze the degradation performance of the hydrogels in vitro. In brief, 20 mg (W_0) samples of dried CHI−OCS hydrogel with different concentration ratios (CHI/OCS = 1:2, 1:1, 2:1, and 4:1) were immersed into 30 mL of PBS (pH = 7.4) at 37 °C, respectively.

At multiple time points, the hydrogel bulks were taken out, washed with deionized water, and weighed again after lyophilization (W_t). All measurements were made using at least 3 replicates. The standard deviation for different data points is shown in the Supporting Information (Table. S2). The degradation ratios of the CHI−OCS hydrogels were calculated according to the following formula

$$\text{Degradation ratio (\%)} = (W_0 - W_t)/W_0 \times 100\%$$

2.14. Cell Live/Dead Staining. The cell viability was evaluated by a Live/Dead cell viability kit (Thermo Fisher Scientific). The extract of CHI−OCS hydrogel with the concentration of 10 mg/mL was made by immersing a hydrogel block of 100 mg into 10 mL of PBS (pH = 7.4) at 37 °C until it degraded completely. PDLSCs and GMSCs were seeded in 24-well plates at a density of 5×10^3/well and cultured for 24 h. Next, 10 μL of extracts was added to each well containing about 500 μL of medium, and cells were incubated for another 1 or 4 days. Then, the samples were stained with calcein-AM (green) and ethidium homodimer (red) on days 1 and 4, respectively, according to the instructions. The cell condition was observed under a fluorescence microscope (EVOS M5000, Thermo Fisher, USA). Six images at least different regions were randomly selected with ImageJ (National Institutes of Health, USA). The number percentage of live cells to dead cells was calculated to represent cell viability.

2.15. Animal. Thirty 8 week old male SD rats were used for animal experiments with the approval from the Laboratory Animal Welfare and Ethics Committee of Zhejiang University (no. ZJU20220034). They were randomly divided to five groups with six rats in each group: the control group, the group of the aligned porous hydrogel (A-HY group), the group of the PDLSC-hydrogel with disordered pores (PDLSC/D-HY group), the group of the PDLSC-aligned porous hydrogel (PDLSC/A-HY group), and the group of the GMSC-aligned porous hydrogel (GMSC/A-HY group). The hydrogel with a concentration of 20 mg/mL at the time of preparation was prepared in advance with the size of 4 mm × 2 mm × 2 mm. During cutting, attention should be paid to the matching of the pore direction of the hydrogel and the implantation direction of the defect. Prepared hydrogels were stored at 4 °C, and hydrogels combined with cells were made fresh at the beginning of each experiment. The PDLSC and GMSC suspensions at a density of 5×10^6 mL maintained in DMEM medium were mixed in the above hydrogel block before implantation. Cells were cultured within the hydrogels in an incubator at 37 °C with 5% CO_2 for 24 h and then collected in EP tubes. Each rat had one defect at a unilateral mandible. The surgical procedure is shown in the Supporting Information (Figure S2). Rats were anesthetized by intraperitoneal injections of sodium pentobarbital (40 mg/kg). The hair of the operating area was shaved, and the skin was disinfected with Betadine. A 2 cm extra-oral incision was made parallel to the lower margin of the mandible to separate the subcutaneous tissue and masseter muscle on the bone surface. The surgical area was irrigated with copious amounts of sterile saline. Using a low-speed hand piece with a diameter round bur, a 4 mm long and 2 mm wide defect was created in the root of the second molar, until the depth reached up to the cementum surface. The defect was located 1 mm below the crest of the alveolar bone, avoiding damaging the tooth root. After 2 rinses in PBS, the samples were implanted in the defect according to the grouping. The masseter muscle and skin were then sutured. Penicillin was injected intraperitoneally (80,000 units/day) for 3 days following the operation. All rats were killed using an overdose of intraperitoneally injected sodium pentobarbital at 1 month after the surgery. Their mandibles were immediately dissected and fixed in 4% PFA. Then, the subsequent experiments were performed.

2.16. Microcomputed Tomography. Mandibular defect samples of rats in each group were scanned by microcomputed tomography (micro-CT, MILabs U-CT-XUHR, Netherlands) at a voltage of 55 kV and a current of 0.17 mA. For each sample, 1440 projections were used, and the scan time was nearly 30 min. The MILabs Reconstruction software (Netherlands) was used to reconstruct the three-dimensional (3D) images, and then, bone volume percentage (bone volume/total volume × 100%, BV/TV × 100%) was analyzed by Imalytics Preclinical (Gremse-IT, Germany) software.

2.17. Histological Staining and Immunohistochemistry. All mandibles were soaked in decalcification solution (0.5 M EDTA, pH = 8) for approximately 2 months. After that, the samples were made into paraffin-embedded sections for hematoxylin and eosin staining (HE), Masson's trichrome staining, and immunohistochemistry. The primary antibodies included the following: mouse anti-osteopontin (OPN) (1:100; Proteintech Group, USA), rabbit anti-Runt-related transcription factor 2 (Runx-2) (1:200; Abways, China), rabbit anti-collagen type I (Col-I) (1:200; Boster, USA), and PBS (negative control). The secondary antibody was a biotin-labeled goat anti-mouse/rabbit IgG complex. Results could be observed with an inverted fluorescence microscope. Five Masson's images and different immunohistochemistry images at least of each group of animals were randomly selected, and the positive area was calculated to represent the expression situation by ImageJ software (National Institutes of Health, USA).

2.18. Statistical Analysis. All quantitative results were analyzed by GraphPad Prism (GraphPad Software, USA) and expressed as means ± standard deviation. Differences between the two groups were analyzed by unpaired Student's *t*-test. Comparisons among groups were achieved by one-way analysis of variance.

3. RESULTS

3.1. Culture, Sorting, and Identification of Human PDLSCs and GMSCs. By using the tissue block digestion method, primary periodontal ligament cells and gingival fibroblasts could become adherent within 7 days (Figure 1A). With being subcultured until the third generation, PDLSCs and GMSCs were isolated by immunomagnetic beads. The isolated cells exhibited a spindle-like morphology (Figure 1A). A CCK8 cell proliferation assay was performed in the above-mentioned cells, and cell proliferation curves were plotted (Figure 1B). On day 3, PDLSCs and GMSCs proliferated rapidly. However, the proliferation viability of PDLSCs was decreased on day 9, while GMSCs reached the proliferative plateau stage on the 11th day. Flow cytometric assay data indicate that both stem cells were positive for the expression of the MSC surface markers CD146, CD105, and Stro-1 and negative for the hematopoietic stem cell marker CD45 expression, as can be seen in Figure 1C. Compared with controls, these multidirectional differentiation assays confirmed that PDLSCs and GMSCs stained positive with Alizarin red and Oil red O after 21 days of osteogenic and adipogenic induction (Figure 1D). Osteogenic expression was more pronounced in PDLSCs, while adipogenic expression was more pronounced in GMSCs. In alkaline phosphatase staining experiment, PDLSCs had a higher expression of ALP compared with PDLSCs. And ALP experiment can be used to discriminate these two cells (Figure 1E).

3.2. Determination of the Oxidization Degree of Chondroitin Sulfate. The CS was oxidized by sodium periodate under light-protected conditions, and then, OCS was prepared. During the oxidation reaction, some glycan chains in CS generated aldehyde groups. The oxidation degree of CS

https://doi.org/10.1021/acsbiomaterials.2c01440
ACS Biomater. Sci. Eng. XXXX, XXX, XXX−XXX

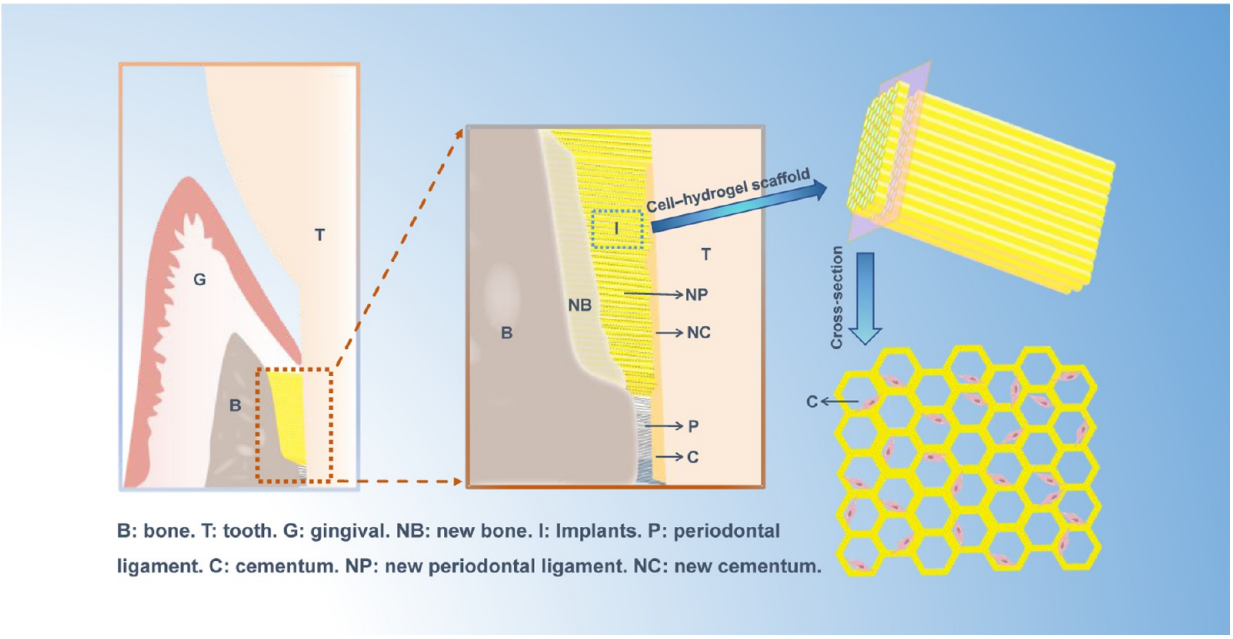

Figure 2. Schematic diagram of the clinical application scenario of the cell-carrying hydrogel scaffold in the treatment of periodontal tissue defects.

can be calculated by the amount of unreacted DNPH for which aldehyde groups can react with DNPH. The standard curve equation of DNPH concentration is shown in the Supporting Information (Figure S1). Meanwhile, the oxidation degree could be controlled via the amount of sodium periodate and oxidation time (Table.1). After reacting with 2.3 g of $NaIO_4$ for 4 h, the oxidation degree of 5 g of CS could reach 20.2%, which we use for other experiments (Figure 2).

3.3. FTIR Spectroscopy Analyses. The FTIR spectra of CHI, CS, OCS, and CHI−OCS hydrogel (HY) are presented in Figure 3. The peak at 1556 cm^{-1} was attributed to the bending

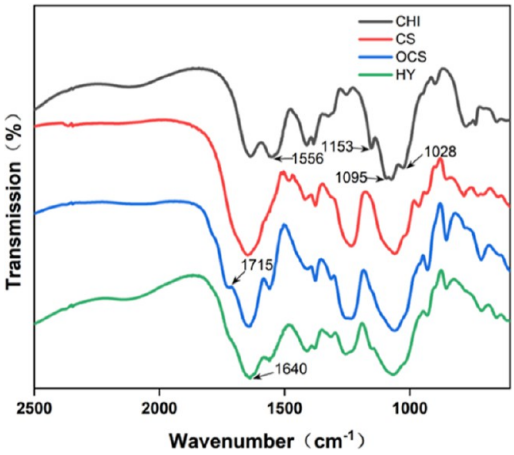

Figure 3. FTIR spectra of CHI, CS, OCS, and CHI−OCS hydrogel.

vibration absorption of amino groups, which was characteristic of CHI. The peaks at 1153, 1095^{-}, and 1028 cm^{-1} could be ascribed to the C−O−C asymmetric stretch vibration and the C−O stretching in CHI. Since CS was successfully oxidized, it had a characteristic peak corresponding to the aldehyde group (−CHO) at 1715 cm^{-1} in FTIR spectra. The occurrence of the Schiff base reaction was clearly demonstrated by the appearance of the characteristic peaks of the imine structure at 1640 cm^{-1} and the disappearance of −CHO in FTIR spectra of the finished hydrogel.

3.4. Swelling and Degradation Characteristics. The ESRs and degradation characteristics were determined by weighing. All the hydrogels expanded dramatically (ESR > 20) in PBS (pH = 7.4) at 37 °C (Figure 4A). However, the ESR decreased with the increasing concentration ratio of CHI, which might be attributed to the increased crosslinking density. The PBS simulated a physiological environment with a pH of 7.4. The degradation values of hydrogels with different concentration ratios of CHI/OCS (1:1, 2:1, and 3:1) were all below 15% after incubation for 8 days. The degradation could reach 98.7, 97.2, 90.1 and 92.9% after incubation for 30 days, respectively. It demonstrated that hydrogels had favorable degradation properties.

3.5. Rheological Property. We evaluated the influence of temperatures on the mechanical behavior of the hydrogels by a rheometer before co-culturing with cells. In response to the temperature increasing from 10 to 40 °C, the values of G' and G'' were relatively stable with some fluctuation (Figure 4B). However, G' (from 1710 to 1200 Pa for hydrogels with the CHI/OCS ratio of 1:1 and from 5970 to 4970 Pa for hydrogels with the ratio of 2:1) was higher than G'' (from 183 to 161 Pa for hydrogels with the ratio of 1:1 and from 1710 to 1200 Pa for hydrogels with the ratio of 2:1) throughout the experiment. This observation indicated that the crosslinked network of Schiff base formation in hydrogels led to predominantly elastic behavior.

3.6. Micromorphology of CHI−OCS Hydrogels. The morphology of CHI−OCS hydrogels was observed in both the transverse section and longitudinal section, as shown in Figure 4D. The significantly porous structure was observed in all samples. The hydrogel showed a honeycomb-like porous network structure, which is more openly aligned along the frozen direction. It had an almost relatively uniform aperture with a mean diameter of 90.13 ± 24.52 μm (SD1), as observed using SEM after the hydrogel was freeze-dried. However, the conventional hydrogel without the freeze-casting treatment did not have the above-mentioned characteristics (Figure 4D),

https://doi.org/10.1021/acsbiomaterials.2c01440
ACS Biomater. Sci. Eng. XXXX, XXX, XXX−XXX

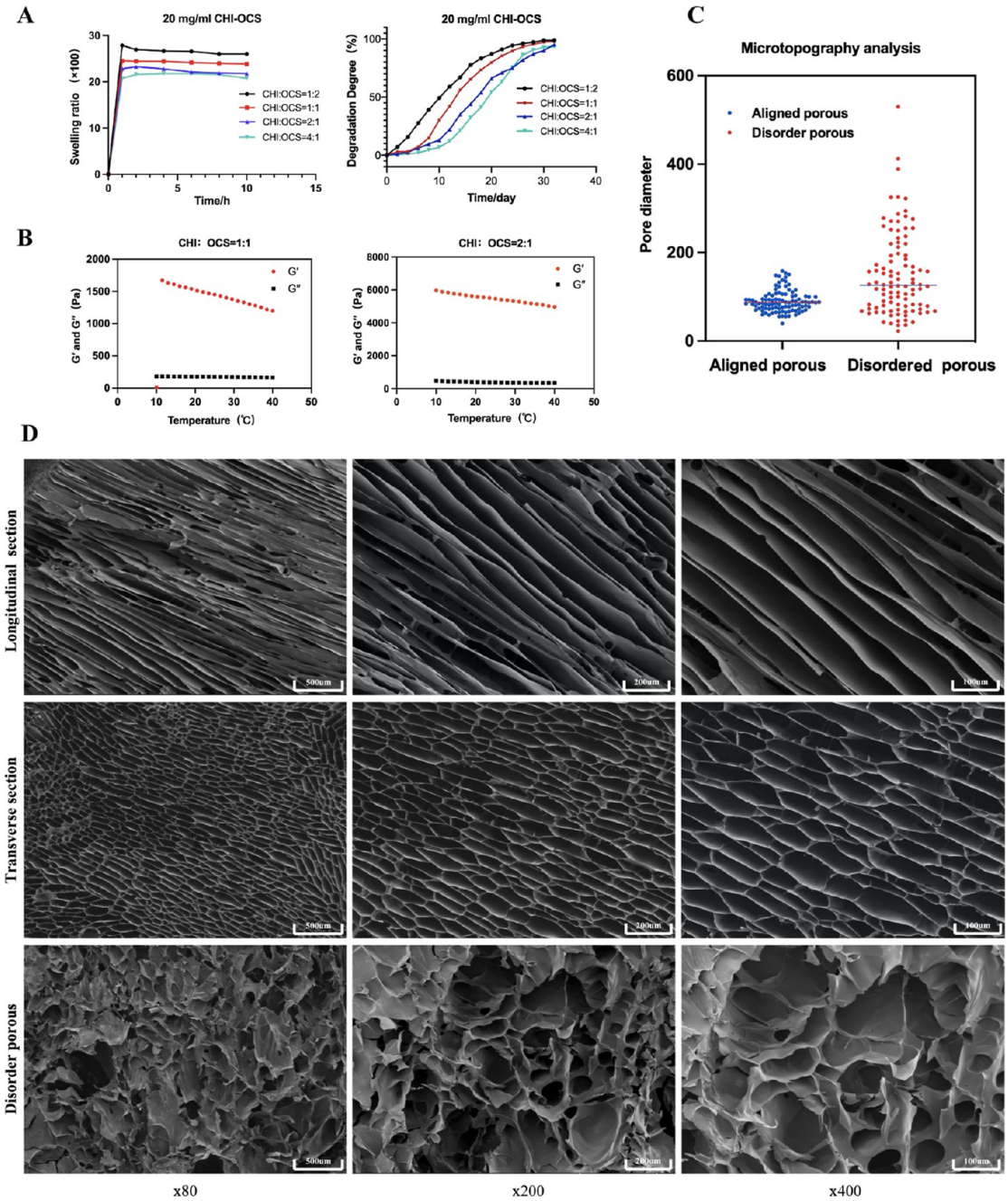

Figure 4. Microscopic morphology and physicochemical properties of CHI−OCS gel. (A) Swelling ratio and degradation degree of different concentration ratios (CHI:OCS = 1:2, 1:1, 2:1, and 4:1) of 20 mg/mL CHI−OCS gel determined by the gravimetric method. (B) Rheological parameters of CHI−OCS gel at two concentrations (CHI:OCS = 1:1 and 2:1). (C) Comparison of the dispersion degree of pore size of CHI−OCS gel with the freeze-casting treatment (90.13 ± 24.52 μm [SD1]) and that of the hydrogel synthesized by the traditional method (149.3 ± 93.50 μm [SD2]). (D) Longitudinal section and transverse section of aligned porous and traditional hydrogel (disorder porous) of CHI−OCS gel were observed by SEM at different magnifications.

whose spherical porous structures are disorderly arranged. The pore size appeared to be heterogeneous in size with an average diameter of 149.3 ± 93.50 μm (SD2). Comparing the standard deviation (SD) values of the two, there was a significant difference in the dispersion of pore sizes (Figure 4C). Therefore, the hydrogel that is aligned and relatively the same size can be obtained with the freeze-casting technique.

3.7. Cytotoxicity Analyses. The results of the live/dead cell staining of PDLSCs and GMSCs that were cultured under hydrogel extracts are exhibited in Figure 5A/5C. PDLSCs and GMSCs had a distinctive proliferative tendency, and no obvious morphological changes were found specially after the two cell types were cultured. When the cells were cultured for 1 and 4 days, no significant difference was noted between the control and experimental group in the survival rate in both PDLSCs and GMSCs. However, when PDLSCs were cultured on the 4th day, the survival rate seemed to decline to some extent. The proliferation of cells cultured under the material is demonstrated in Figure 5B/5D. For both types of cells, there was no statistical difference in cell viability between the experimental group and control group at 1, 3, 5, and 7 days. Cell viability was significantly decreased only in the experimental group (PDLSC-HY group)

https://doi.org/10.1021/acsbiomaterials.2c01440
ACS Biomater. Sci. Eng. XXXX, XXX, XXX−XXX

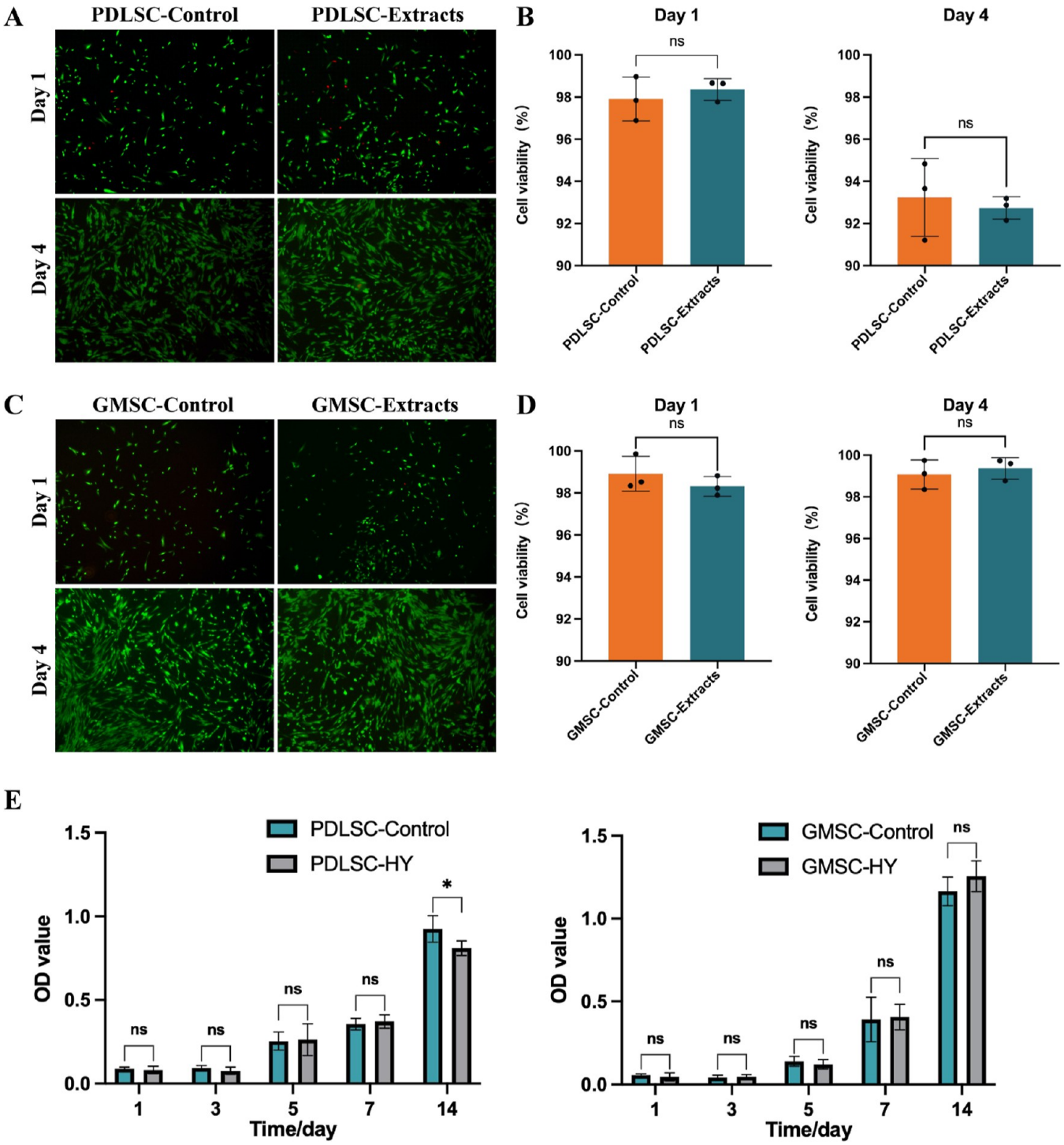

Figure 5. Hydrogel biocompatibility assessment. (A) PDLSCs were cultured under cell extracts, and live/dead cells were stained after 1 and 4 days. (B) Comparison of cell viability after live/dead cell staining after culturing PDLSCs under cell extracts at 1 and 4 days. (C) GMSCs were cultured under cell extract and live/dead cells were stained after 1 and 4 days. (D) Comparison of cell viability after live/dead cell staining after culturing GMSCs under cell extracts at 1 and 4 days. (E) Proliferation situation of PDLSCs and GMSCs at 1, 3, 5, 7, and 14 days. Statistically significant differences are marked as ns (no significance) and *($P < 0.05$).

at 14 days compared to that in the PDLSC group ($P < 0.05$), which was not observed in the GMSC group. The results of live/dead staining and CCK8 indicated that CHI−OCS hydrogels had good biocompatibility and low toxicity.

3.8. Microcomputed Tomography Analysis. The mandibles were analyzed by micro-CT 4 weeks after surgery (Figure 6A). The control group indicated fewer signs of repair, while the four groups with implants showed different levels of bone regeneration. Among the four groups with implants, the A-HY group had the least improvement in bone density. Although the surfaces of the PDLSC/D-HY group, PDLSC/A-HY group, and GMSC/A-HY group could be seen as rough and pitted on the bone surface, the root of the tooth is more evidently covered by the new bone (high density). According to quantitative BV/

https://doi.org/10.1021/acsbiomaterials.2c01440
ACS Biomater. Sci. Eng. XXXX, XXX, XXX−XXX

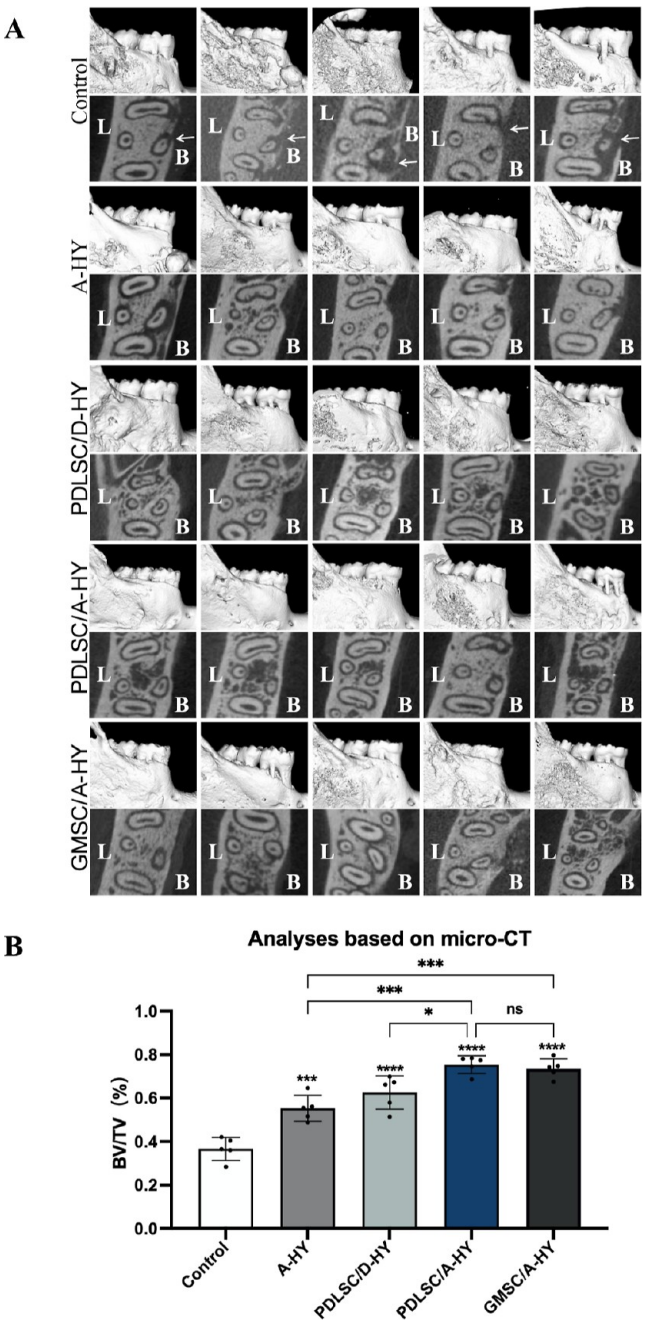

Figure 6. Micro-CT 3D analysis of mandibular bone in rats a with periodontal defect 1 month after the operation. (A) 3D reconstruction and horizontal section images of the mandible with a periodontal tissue defect (white arrows indicate the alveolar bone that does not fully cover the root surface). Groups: control group (control), group of aligned porous hydrogel (A-HY), group of PDLSC-hydrogel with disordered pores (PDLSC/D-HY), group of PDLSC-aligned porous hydrogel (PDLSC/A-HY), and group of GMSC-aligned porous hydrogel (GMSC/A-HY). L: lingual and B: buccal. (B) Quantitative BV/TV (%) analyses of all groups based on micro-CT. Statistically significant differences are marked as ns (no significance), *($P < 0.05$), **($P < 0.01$), ***($P < 0.001$), and ****($P < 0.0001$).

TV analysis (Figure 6B), the A-HY group (55.33 ± 5.98%), PDLSC/D-HY group (62.53 ± 7.66%), PDLSC/A-HY group (75.39 ± 4.06%), and GMSC/A-HY group (73.63 ± 4.45%) showed a more pronounced bone tissue repair than the control group (36.69 ± 5.29%) at 4 weeks ($P < 0.05$). Furthermore, statistically significant differences between the A-HY group and PDLSC/A-HY group ($P < 0.001$), the PDLSC/D-HY group and PDLSC/A-HY group ($P < 0.05$), and the A-HY group and GMSC/A-HY group ($P < 0.001$) were indicated, whereas that between the PDLSC/A-HY group and GMSC/A-HY group was not observed ($P > 0.05$). Micro-CT analysis showed that compared with the control group, the implants in each group can promote bone regeneration in vivo. Besides, the promotion effect of hydrogel combined with PDLSCs/GMSCs was better than that of hydrogel alone. Also, the effect of the directional porous hydrogel was better than that of traditional hydrogel synthesis.

3.9. Animal Tissue Staining. HE-stained images illustrated that 1 month after the operation, the formation of new cementum-like tissue (NC-like tissue) was observed on the root surfaces of the mandibular second molars of rats in each group (Figure 7A). The continuous laminar structure was not formed in the NC-like tissue of the control group, however, which was formed in the A-HY group, the PDLSC/D-HY group, the GMSC/A-HY group, and especially the PDLSC/A-HY group. Masson's trichrome images showed the arrangement direction, distribution, and density of the new periodontal ligament-like tissue (NP-like tissue) (Figure 7A). The NP-like tissue of high density was formed between the surface of the formed bone tissue and the tooth root surface in the A-HY group ($P < 0.001$), PDLSC/D-HY group ($P < 0.01$), PDLSC/A-HY group ($P < 0.0001$), and GMSC/A-HY group ($P < 0.0001$) compared to the control group (Figure 7B). The arrangement of NP-like tissue formed in the PDLSC/D-HY group was more cluttered than that of the other groups (Figure 7A). The regeneration of periodontal fibrous tissue was not obvious in the control group. HE staining and Masson's trichrome analysis indicated that the implantation of the hydrogel contributes to the regeneration of NP-like tissue and NC-like tissue, and the aligned porous hydrogel is more conducive to the order growth of periodontal ligament.

Immunohistochemistry-positive staining of OPN and Runx-2 could be tested in the new tissue of the periodontal bone defect (NB-like tissue) on the root surface (Figure 8A). The OPN and Runx-2 expressions in the A-HY group, PDLSC/D-HY group, PDLSC/A-HY group, and GMSC/A-HY group were more apparent than that in the control group ($P < 0.01$) (Figure 8B/8C). Furthermore, COL-I could be detected in new fibrous tissue, normal periodontal ligament fibers, and mineralized bone tissue in each group (Figure 8). The PDLSC/D-HY group, PDLSC/A-HY group, and GMSC/A-HY group showed higher expressions than the control group and A-HY group (Figure 8D). The expression of osteogenic and fibroblast-related factors indicated that the hydrogel implantation groups had different promoting effects on periodontal regeneration.

4. DISCUSSION

Many studies had indicated that it was feasible to carry stem cells using hydrogels as scaffold materials to promote tissue repair. Hydrogels with different characteristics have been widely studied and applied in various fields, especially in the field of bone regeneration.[36,37] In this study, an aligned porous hydrogel material was used as a carrier to ensure better nutrition and gas exchange of stem cells. Previous studies have shown that PDLSCs and GMSCs can release paracrine growth factors, cytokines, etc. to the surrounding environment, which can enhance the regeneration ability of periodontal tissue.[38,39] Besides, their functions include immune regulation, promoting

https://doi.org/10.1021/acsbiomaterials.2c01440
ACS Biomater. Sci. Eng. XXXX, XXX, XXX−XXX

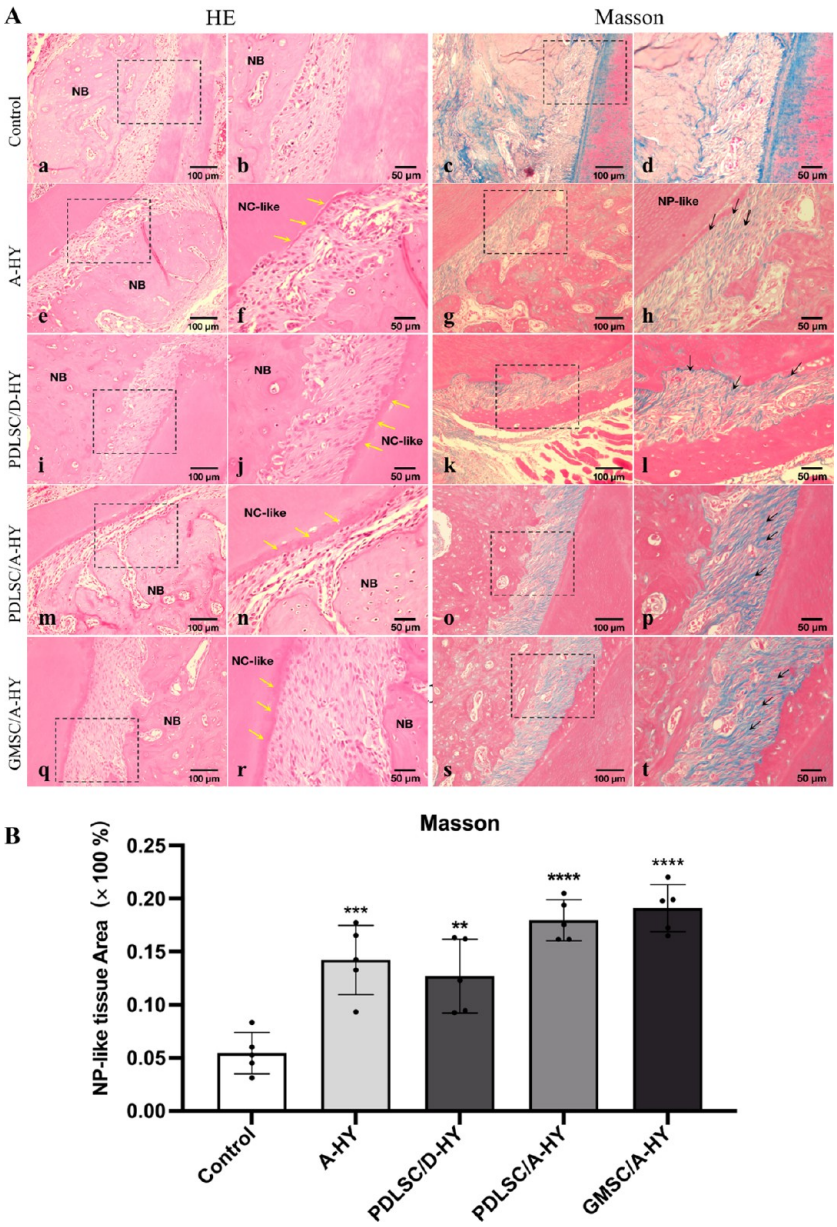

Figure 7. Histology illustration images and statistical analysis of the periodontal defect of the rat mandibular second molar at 1 month postoperatively are shown. (A) (a), (b), (e), (f), (i), (j), (m), (n), (q), and (r) are HE images, and (c), (d), (g), (h), (k), (l), (o), (p), (s), and (t) are Masson's trichrome images, where (b), (f), (j), (n), (r), (d), (h), (l), (p), and (t) are high-magnification images corresponding to the dotted frame on the left. Yellow arrow: new cementum-like: the direction of the new PDL-like tissues on the root surface. NB: new bone. NC-like: new cementum-like tissues. Black arrow: NP-like tissues. NP-like: new periodontal ligament-like tissues. (B) Percentage of Masson's trichrome staining positive area. Statistically significant differences are marked as **($P < 0.01$), ***($P < 0.001$), and ****($P < 0.0001$).

angiogenesis, anti-apoptosis, chemoattraction, etc., which might benefit tissue regeneration too.[40,41] Therefore, these two MSCs will be loaded in the aligned porous hydrogel and transplanted into the periodontal tissue defect area of rats to verify the feasibility of promoting tissue regeneration.

The primary cells were obtained from the periodontal ligament and gingival tissue by the tissue block method. PDLSCs and GMSCs were obtained after isolation and purification by the immunomagnetic bead method for flow cytometry phenotype analysis. The results showed that PDLSCs and GMSCs were positive for the expression of MSC markers CD146, CD105, and Stro-1 and negative for the expression of the hematopoietic stem cell marker CD45. PDLSCs are superior to GMSCs in osteogenic differentiation, but the opposite is true in adipogenic differentiation. PDLSCs have a higher expression than GMSCs in both osteogenic differentiation and ALP experiment, which represent osteogenic activity. In addition, the cell proliferation activity of GMSCs is stronger than that of PDLSCs, which was verified in CCK8 and live/dead cell staining experiments. Compared with PDLSCs whose proliferative activity decreased on the 9th day, GMSCs could reach a platform stage on the 11th day without significant attenuation. Similar results that GMSCs have a shorter doubling time than PDLSCs have been expressed in the study of Hao Yang et al.[25]

In this study, we used DNPH titration to measure the degree of oxidation of CS under different oxidation conditions to explore the properties of hydrogels formed by different degrees of oxidation of CS in subsequent studies. The reaction groups of

https://doi.org/10.1021/acsbiomaterials.2c01440
ACS Biomater. Sci. Eng. XXXX, XXX, XXX−XXX

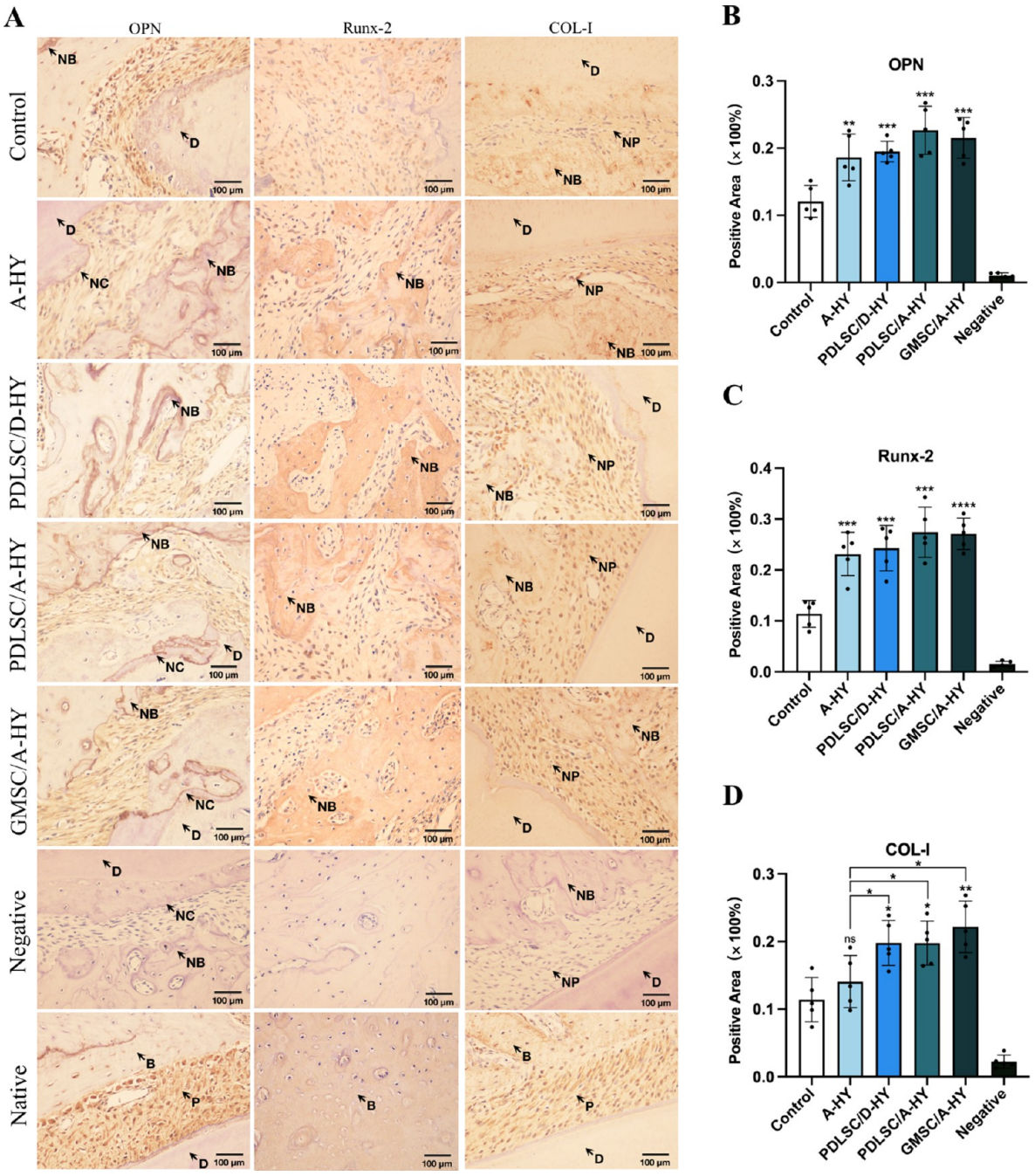

Figure 8. Immunohistochemistry images and statistical analysis of the periodontal defect of the rat mandibular second molar at 1 month postoperatively are shown. (A) Black arrows show the staining of OPN, Runx-2, or Col-I in control, A-HY, PDLSC/D-HY, PDLSC/A-HY, and GMSC/A-HY groups, and negative control (negative). The positive control of a natural tooth adjacent to an experiment site (native). NB: new bone. B: bone. NC: new cementum. C: cementum. NP: new periodontal ligament. P: periodontal ligament. D: dentin. (B) Percentage of the OPN positive area. (C) Percentage of the Runx-2 positive area. (D) Percentage of the COL-I positive area. Statistically significant differences are marked as ns (no significance), *($P < 0.05$), **($P < 0.01$), ***($P < 0.001$), and ****($P < 0.0001$).

the substrates (CHI, CS, and OCS) were identified by FTIR spectra, and the gelling reaction between OCS and CHI was determined to be due to the Schiff base reaction according to the changes of the characteristic peaks before and after the reaction. These conclusions are the same as those of the previous research of Hongbin Li et al.,[42] and the degree of oxidation of CS (degree of aldehyde substitution) is controllable and adjustable. Our experiment showed that the higher oxidation degree of OCS led to faster gelation after the directional freezing treatment and transfer to a −8 °C freezer. The hydrogels with an oxidation degree of 20.2% OCS formed in 2−3 days, while the hydrogels with an oxidation degree of 9.3% needed at least 7 days. So, OCS with the oxidation degree of 20.2% was chosen to prepare the hydrogel. The hydrogels meeting the experimental requirements could be synthesized in a shorter time by choosing the former. Through the study on the swelling and degradation properties of hydrogels by the weighing method, we know that hydrogels with different preparation concentration ratios can quickly reach the swelling equilibrium with the ESR of all of the hydrogels over 20 in PBS (pH = 7.4) at 37 °C, but the swelling ratio between them

https://doi.org/10.1021/acsbiomaterials.2c01440
ACS Biomater. Sci. Eng. XXXX, XXX, XXX−XXX

is slightly different. Hydrogels with a higher CHI ratio had a smaller swelling ratio. In the degradation performance study, the degradation degree of the hydrogel with the concentration ratio of CHI to OCS of 1:1, 2:1, and 4:1 was less than 15% in the first 8 days, but it was almost completely degraded after 30 days. This ensures that when the hydrogel is used as the carrier for stem cell implantation, the implant can maintain the original pore structure in the early stage and support the stem cells to play a role in certain periods. After that, it can be almost completely degraded, avoiding the possible immunogen reaction of the grafts to the greatest extent, although the biocompatibility of CHI and CS is superior.[8−12,14,15,43] The rheological property test of the hydrogel in the temperature range of 10 to 40 °C showed that the hydrogel had a certain mechanical strength after preparation. So, the temperature conditions of its conventional storage, transportation, and implantation did not significantly change its mechanical properties. Notably, the hydrogels with a higher CHI ratio (2/3) had a higher value of G' and G'' in the presence of the same concentration (20 mg/mL), which exhibited a stronger mechanical performance. The changing characteristics of the mechanical properties and swelling ratio of hydrogels may be due to the higher crosslinking density of hydrogels with more CHI as the substrate and the decreased water absorption capacity.[35] There have been a large number of studies on hydrogels as biomaterials in the past. In recent years, more and more freeze-casting biomaterials have been prepared with the order pore size and direction as the main technical means. This research is the first attempt to apply an aligned porous hydrogel scaffold combined with stem cells in periodontal tissue regeneration. CHI and CS were selected as substrates to realize the construction of the aligned porous hydrogel in our research. According to the SEM image and analysis of pore size, we know that the pore direction is relatively ordered, and the average pore size of the hydrogel after directional freezing treatment is 90.13 ± 24.52 μm, while the average pore diameter of ordinary hydrogel is 149.3 ± 93.50 μm. The diameters of the two kinds of MSCs are about 10−50 μm, which can result in nutrition and gas exchange that are necessary for proliferation and differentiation.

At present, hydrogels have been widely used as biological regeneration materials, cell scaffolds, etc. For scaffold materials, in addition to the necessary mechanical properties, swelling and degradation properties, and pore structure, good biological activity is also a top priority. We chose CHI and CS as substrates to ensure the superior biocompatibility of the scaffold materials. The results of CCK8 and live/dead cell staining experiments in multiple groups indicated that there was no significant difference in cell viability between the hydrogel group and the control group. We learned that CHI−OCS hydrogel co-cultured with cells and its degradation extract did not affect the cell activity and had good biocompatibility. Therefore, we continued to carry out animal experiments.

The defective bone tissue provides space for hydrogel implantation. While constructing the periodontal defect model, we created a rigid space wrapped by bone tissue and tooth tissue by surgery to maintain the hydrogel in the operation area. We cut the hydrogel according to the defect space and made the aperture direction perpendicular to the root surface while implanting it. We implanted the cells and hydrogel into the rats with periodontal defect models after co-culture so that the hydrogel material can completely cover the root surface, fill the defect area, and closely suture. One month after the surgery, micro-CT results showed that compared with the control group, the implants in each group had a promoting effect on bone regeneration in the periodontal defect area. The A-HY group was statistically different compared with the PDLSC/A-HY group ($P < 0.001$) and GMSC/A-HY group ($P < 0.001$), indicating that the promoting effect of hydrogel co-cell implantation was better than that of the hydrogel alone. Moreover, there is a statistical difference between the PDLSC/D-HY group and PDLSC/A-HY group ($P < 0.05$), indicating that the effect of the aligned porous hydrogel is better than that of traditional hydrogel synthesis. In addition to micro-CT, we also carried out verification of multiple dimensions, including HE staining and Masson's trichrome staining. HE staining showed that compared with the control group, each group with implants had different degrees of NC-like structure deposition, and Masson's trichrome stain showed high-density NP-like tissue formation. From the images, we know that the PDLSC/A-HY group formed the most continuous and complete cementum on the root surface, and the high-density NP-like tissue of the PDLSC/D-HY group was different from that of other groups in an orderly arrangement but more disordered. It is proved that the A-HY group ($P < 0.001$), PDLSC/D-HY group ($P < 0.01$), PDLSC/A-HY group ($P < 0.0001$), and GMSC/A-HY group ($P < 0.0001$) formed high-density NP-like tissue by the analysis of the percentage of Masson's trichrome staining positive area.

In immunohistochemistry positive staining experiment, the osteogenesis-related markers OPN and Runx-2 were highly expressed in the A-HY group, PDLSC/D-HY group, PDLSC/A-HY group, and GMSC/A-HY group ($P < 0.05$). And Col-I markers were detected in the PDLSC/D-HY group, PDLSC/A-HY group, and GMSC/A-HY group ($P < 0.05$) in the new fibrous tissues and mineralized bone tissues. In addition, after dissecting and separating the rat mandible 1 month after the operation, we paid attention to the degradation of the implants in the rat body. All implants in the mandibular defect area of the rat were no longer visible or still had a little adhesion with the new tissue, and no immune rejection was found in the staining section. The results of animal experiments suggested that it is feasible and effective to use hydrogel as a biological scaffold to carry stem cells and implant them into the defect area to treat periodontal tissue defects.

Significantly, our results of micro-CT analysis and tissue staining showed that there is a difference between PDLSC/A-HY and PDLSC/D-HY. Previous literature studies reported that cells can transmit the necessary nutrients, oxygen, growth factors, etc. through the microporous network between the pore structures of the scaffold materials, which is essential to maintain the cell vitality and function for a long time.[44] Besides, both the architecture (morphology and pore size distribution) and the pore size of scaffold materials play an important role in the formation of new tissue in growth. Scaffolds with a high number of homogeneous pore size allows cells a faster colonization.[45] It was valid to consider that disordered hydrogels reduced the diffusion of nutrients and oxygen and cellular waste and further influenced the regenerative effect of stem cells. So, controlling the size and direction of the hydrogel aperture to a certain extent may be meaningful for the regeneration and repair of periodontal tissue defects, especially periodontal ligament defects. In our study, there was a difference in the ability of regeneration and differentiation between the two in vitro conditions. PDLSCs are superior to GMSCs in osteogenic differentiation, which is the focus of our attention in animal experiments. However, many studies have proved that aside

https://doi.org/10.1021/acsbiomaterials.2c01440
ACS Biomater. Sci. Eng. XXXX, XXX, XXX−XXX

from the well-established self-renewal and multipotent differentiation properties, GMSCs exhibit both immunomodulatory and anti-inflammatory roles in several experimental autoimmune and inflammatory diseases.[27−31,46] For example, GMSCs markedly increased the numbers of interleukin (IL)-10^+ regulatory T cells, reduced the secretion of pro-inflammatory cytokines, and increased the production of anti-inflammatory cytokines.[47] Extracellular vesicles derived from GMSCs stimulated with TNF-α and IFN-α promote M2 macrophage polarization via enhanced CD73 and CD5L expression.[48] So, we considered that the differences in the regenerative ability of the two types of stem cells were not reflected in the in vivo environment because of the interference of many factors such as inflammation in the periodontal tissue. Therefore, the results of animal experiments using PDLSCs and GMSCs are almost the same, which are both excellent candidate seed cells for periodontal tissue engineering. And the application potential of GMSCs, which are easier to obtain and have a shorter multiplication time in vitro, deserves more attention and exploration. In the absence of cells, although the effect of promoting regeneration of pure hydrogel as an implant is not ideal, it still has positive significance. This may be attributed to the implantation of scaffold materials providing a certain space for periodontal tissue regeneration.[49]

In conclusion, our study preliminarily verified the potential of PDLSCs and GMSCs to promote periodontal regeneration, which were delivered to the periodontal defect area with aligned porous hydrogel treated by the freeze-casting technique as the carrier. It provides a new direction for the treatment of periodontal tissue defects.

5. CONCLUSIONS

PDLSCs and GMSCs sorted by tissue block immunomagnetic beads have the characteristics of MSCs, which can be used for periodontal tissue regeneration engineering because of their multi-differentiation ability. GMSCs are inferior to PDLSCs in osteogenic differentiation in vitro, while their proliferation and differentiation abilities are better. The OCS can react with CHI to form a hydrogel by the Schiff base reaction, and the CHI−OCS hydrogel treated by freezing-casting met the requirements of carrying cells in terms of micromorphology and physical and chemical properties and had good biocompatibility and low cytotoxicity.

CHI−OCS−PDLSC/GMSC hydrogel has a good effect on promoting tissue regeneration in rat periodontal defect models, and there is no obvious immune response, which can be used for tissue regeneration engineering.

■ ASSOCIATED CONTENT

Supporting Information

The Supporting Information is available free of charge at https://pubs.acs.org/doi/10.1021/acsbiomaterials.2c01440.

Standard concentration curve of DNPH; standard deviation of swelling ratio data for different data points; standard deviation of degradation degree data for different data points; pore diameter of aligned porous and disordered porous hydrogel (μm); and the operation process of the rat periodontal bone defect model, including (a) shaving and exposing the operation area, (b) cutting the skin after disinfection, (c) separating the mucosa, muscle layer, and periosteum to expose the bone surface, (d) preparation of the mandibular bone defect, (e) directional implantation of materials, and (f) suturing the wound hierarchically and intermittently (PDF)

■ AUTHOR INFORMATION

Corresponding Author

Yanmin Wu − *Department of Periodontology, the Second Affiliated Hospital, College of Medicine, Zhejiang University, Hangzhou 310000, People's Republic of China*; Email: wuyanmin@zju.edu.cn

Authors

Wenhao Wang − *Department of Periodontology, the Second Affiliated Hospital, College of Medicine, Zhejiang University, Hangzhou 310000, People's Republic of China; Key Laboratory of Oral Biomedical Research of Zhejiang Province, Zhejiang University School of Stomatology, Hangzhou 310000, People's Republic of China*; orcid.org/0000-0003-3053-3054

Ao Wang − *Department of Periodontology, the Second Affiliated Hospital, College of Medicine, Zhejiang University, Hangzhou 310000, People's Republic of China; Key Laboratory of Oral Biomedical Research of Zhejiang Province, Zhejiang University School of Stomatology, Hangzhou 310000, People's Republic of China*

Gaofu Hu − *Department of Periodontology, the Second Affiliated Hospital, College of Medicine, Zhejiang University, Hangzhou 310000, People's Republic of China*

Mengyao Bian − *Department of Periodontology, the Second Affiliated Hospital, College of Medicine, Zhejiang University, Hangzhou 310000, People's Republic of China*

Lili Chen − *Department of Periodontology, the Second Affiliated Hospital, College of Medicine, Zhejiang University, Hangzhou 310000, People's Republic of China*; orcid.org/0000-0002-0620-8844

Qian Zhao − *State Key Laboratory of Chemical Engineering, College of Chemical and Biological Engineering, Zhejiang University, Hangzhou 310000, People's Republic of China; ZJU-Hangzhou Global Scientific and Technological Innovation Center, Hangzhou 310000, People's Republic of China*; orcid.org/0000-0002-6931-9859

Weilian Sun − *Department of Periodontology, the Second Affiliated Hospital, College of Medicine, Zhejiang University, Hangzhou 310000, People's Republic of China*

Complete contact information is available at: https://pubs.acs.org/10.1021/acsbiomaterials.2c01440

Author Contributions

W.W. and W.A. contributed equally to this paper. W.Y. and S.W. contributed equally to this paper. The manuscript was written through contributions of all authors. All authors have given approval to the final version of the manuscript.

Notes

The authors declare no competing financial interest.

■ ACKNOWLEDGMENTS

We would like to thank Dr. Yao Jiang from the Department of Periodontology, Stomatology Hospital of Zhejiang University School of Medicine, (Hangzhou, China) for her help in modifying the manuscript. This research was supported by grants from the Provincial Key Research and Development Project of Zhejiang (2019C03027), a project supported by the Scientific Research Fund of Zhejiang University (XY2021029),

and the Basic Public Welfare Research Program of Zhejiang Province, China (LTGY23H140005).

REFERENCES

(1) Tobita, M.; Mizuno, H. Periodontal Disease and Periodontal Tissue Regeneration. *CSCR* **2010**, *5*, 168−174.

(2) Hamedi, H.; Moradi, S.; Hudson, S. M.; Tonelli, A. E. Chitosan Based Hydrogels and Their Applications for Drug Delivery in Wound Dressings: A Review. *Carbohydr. Polym.* **2018**, *199*, 445−460.

(3) Dubey, N.; Ferreira, J. A.; Daghrery, A.; Aytac, Z.; Malda, J.; Bhaduri, S. B.; Bottino, M. C. Highly Tunable Bioactive Fiber-Reinforced Hydrogel for Guided Bone Regeneration. *Acta Biomater.* **2020**, *113*, 164−176.

(4) Ammar, M. M.; Waly, G. H.; Saniour, S. H.; Moussa, T. A. Growth Factor Release and Enhanced Encapsulated Periodontal Stem Cells Viability by Freeze-Dried Platelet Concentrate Loaded Thermo-Sensitive Hydrogel for Periodontal Regeneration. *Saudi Dent J* **2018**, *30*, 355−364.

(5) He, X.-T.; Li, X.; Xia, Y.; Yin, Y.; Wu, R.-X.; Sun, H.-H.; Chen, F.-M. Building Capacity for Macrophage Modulation and Stem Cell Recruitment in High-Stiffness Hydrogels for Complex Periodontal Regeneration: Experimental Studies in Vitro and in Rats. *Acta Biomater.* **2019**, *88*, 162−180.

(6) Wang, H.; Wu, G.; Zhang, J.; Zhou, K.; Yin, B.; Su, X.; Qiu, G.; Yang, G.; Zhang, X.; Zhou, G.; Wu, Z. Osteogenic Effect of Controlled Released RhBMP-2 in 3D Printed Porous Hydroxyapatite Scaffold. *Colloids Surf B Biointerfaces* **2016**, *141*, 491−498.

(7) Sowmya, S.; Mony, U.; Jayachandran, P.; Reshma, S.; Kumar, R. A.; Arzate, H.; Nair, S. V.; Jayakumar, R. Tri-Layered Nanocomposite Hydrogel Scaffold for the Concurrent Regeneration of Cementum, Periodontal Ligament, and Alveolar Bone. *Adv Healthc Mater* **2017**, *6*(). DOI: 10.1002/adhm.201601251.

(8) Pellá, M. C. G.; Lima-Tenório, M. K.; Tenório-Neto, E. T.; Guilherme, M. R.; Muniz, E. C.; Rubira, A. F. Chitosan-Based Hydrogels: From Preparation to Biomedical Applications. *Carbohydr. Polym.* **2018**, *196*, 233−245.

(9) Shahzadi, L.; Bashir, M.; Tehseen, S.; Zehra, M.; Mehmood, A.; Chaudhry, A. A.; Rehman, I. U.; Yar, M. Thyroxine Impregnated Chitosan-Based Dressings Stimulate Angiogenesis and Support Fast Wounds Healing in Rats: Potential Clinical Candidates. *Int. J. Biol. Macromol.* **2020**, *160*, 296−306.

(10) Li, J.; Wu, Y.; Zhao, L. Antibacterial Activity and Mechanism of Chitosan with Ultra High Molecular Weight. *Carbohydr. Polym.* **2016**, *148*, 200−205.

(11) Naskar, S.; Kuotsu, K.; Sharma, S. Chitosan-Based Nanoparticles as Drug Delivery Systems: A Review on Two Decades of Research. *J Drug Target* **2019**, *27*, 379−393.

(12) Mikami, T.; Kitagawa, H. Biosynthesis and Function of Chondroitin Sulfate. *Biochim. Biophys. Acta* **2013**, *1830*, 4719−4733.

(13) Shin, J.; Kang, E. H.; Choi, S.; Jeon, E. J.; Cho, J. H.; Kang, D.; Lee, H.; Yun, I. S.; Cho, S.-W. Tissue-Adhesive Chondroitin Sulfate Hydrogel for Cartilage Reconstruction. *ACS Biomater Sci Eng* **2021**, *7*, 4230−4243.

(14) Yang, J.; Shen, M.; Wen, H.; Luo, Y.; Huang, R.; Rong, L.; Xie, J. Recent Advance in Delivery System and Tissue Engineering Applications of Chondroitin Sulfate. *Carbohydr. Polym.* **2020**, *230*, 115650.

(15) Li, C.; Wang, K.; Zhou, X.; Li, T.; Xu, Y.; Qiang, L.; Peng, M.; Xu, Y.; Xie, L.; He, C.; Wang, B.; Wang, J. Controllable Fabrication of Hydroxybutyl Chitosan/Oxidized Chondroitin Sulfate Hydrogels by 3D Bioprinting Technique for Cartilage Tissue Engineering. *Biomed. Mater.* **2019**, *14*, 025006.

(16) Dawlee, S.; Sugandhi, A.; Balakrishnan, B.; Labarre, D.; Jayakrishnan, A. Oxidized Chondroitin Sulfate-Cross-Linked Gelatin Matrixes: A New Class of Hydrogels. *Biomacromolecules* **2005**, *6*, 2040−2048.

(17) Zhou, L.; Fan, L.; Zhang, F.-M.; Jiang, Y.; Cai, M.; Dai, C.; Luo, Y.-A.; Tu, L.-J.; Zhou, Z.-N.; Li, X.-J.; Ning, C.-Y.; Zheng, K.; Boccaccini, A. R.; Tan, G.-X. Hybrid Gelatin/Oxidized Chondroitin Sulfate Hydrogels Incorporating Bioactive Glass Nanoparticles with Enhanced Mechanical Properties, Mineralization, and Osteogenic Differentiation. *Bioact Mater* **2021**, *6*, 890−904.

(18) Kim, J.-E.; Takanche, J.-S.; Yun, B.-S.; Yi, H.-K. Anti-Inflammatory Character of Phelligridin D Modulates Periodontal Regeneration in Lipopolysaccharide-Induced Human Periodontal Ligament Cells. *J Periodontal Res* **2018**, *53*, 816−824.

(19) Eleuterio, E.; Trubiani, O.; Sulpizio, M.; Di Giuseppe, F.; Pierdomenico, L.; Marchisio, M.; Giancola, R.; Giammaria, G.; Miscia, S.; Caputi, S.; Di Ilio, C.; Angelucci, S. Proteome of Human Stem Cells from Periodontal Ligament and Dental Pulp. *PLoS One* **2013**, *8*, No. e71101.

(20) Nyman, S.; Gottlow, J.; Karring, T.; Lindhe, J. The Regenerative Potential of the Periodontal Ligament. An Experimental Study in the Monkey. *J Clin Periodontol* **1982**, *9*, 257−265.

(21) Kim, D.; Lee, A. E.; Xu, Q.; Zhang, Q.; Le, A. D. Gingiva-Derived Mesenchymal Stem Cells: Potential Application in Tissue Engineering and Regenerative Medicine - A Comprehensive Review. *Front Immunol* **2021**, *12*, 667221.

(22) Fawzy El-Sayed, K. M.; Dörfer, C. E. Gingival Mesenchymal Stem/Progenitor Cells: A Unique Tissue Engineering Gem. *Stem Cells Int* **2016**, *2016*, 1.

(23) Fournier, B. P. J.; Larjava, H.; Häkkinen, L. Gingiva as a Source of Stem Cells with Therapeutic Potential. *Stem Cells Dev* **2013**, *22*, 3157−3177.

(24) Farhat, W.; Hasan, A.; Lucia, L.; Becquart, F.; Ayoub, A.; Kobeissy, F. Hydrogels for Advanced Stem Cell Therapies: A Biomimetic Materials Approach for Enhancing Natural Tissue Function. *IEEE Rev Biomed Eng* **2019**, *12*, 333−351.

(25) Yang, H.; Gao, L.-N.; An, Y.; Hu, C.-H.; Jin, F.; Zhou, J.; Jin, Y.; Chen, F.-M. Comparison of Mesenchymal Stem Cells Derived from Gingival Tissue and Periodontal Ligament in Different Incubation Conditions. *Biomaterials* **2013**, *34*, 7033−7047.

(26) Liu, H.; Li, D.; Zhang, Y.; Li, M. Inflammation, Mesenchymal Stem Cells and Bone Regeneration. *Histochem. Cell Biol.* **2018**, *149*, 393−404.

(27) Zhang, X.; Huang, F.; Li, W.; Dang, J.-L.; Yuan, J.; Wang, J.; Zeng, D.-L.; Sun, C.-X.; Liu, Y.-Y.; Ao, Q.; Tan, H.; Su, W.; Qian, X.; Olsen, N.; Zheng, S. G. Human Gingiva-Derived Mesenchymal Stem Cells Modulate Monocytes/Macrophages and Alleviate Atherosclerosis. *Front Immunol* **2018**, *9*, 878.

(28) Nakao, Y.; Fukuda, T.; Zhang, Q.; Sanui, T.; Shinjo, T.; Kou, X.; Chen, C.; Liu, D.; Watanabe, Y.; Hayashi, C.; Yamato, H.; Yotsumoto, K.; Tanaka, U.; Taketomi, T.; Uchiumi, T.; Le, A. D.; Shi, S.; Nishimura, F. Exosomes from TNF-α-Treated Human Gingiva-Derived MSCs Enhance M2 Macrophage Polarization and Inhibit Periodontal Bone Loss. *Acta Biomater.* **2021**, *122*, 306−324.

(29) Zhang, Y.; Wang, Z.; Shi, B.; Li, Y.; Wang, R.; Sun, J.; Hu, Y.; Yuan, C.; Xu, Q. Effect of Gingival Mesenchymal Stem Cell-Derived Exosomes on Inflammatory Macrophages in a High-Lipid Micro-environment. *Int. Immunopharmacol.* **2021**, *94*, 107455.

(30) Wang, R.; Ji, Q.; Meng, C.; Liu, H.; Fan, C.; Lipkind, S.; Wang, Z.; Xu, Q. Role of Gingival Mesenchymal Stem Cell Exosomes in Macrophage Polarization under Inflammatory Conditions. *Int. Immunopharmacol.* **2020**, *81*, 106030.

(31) Górski, B. Gingiva as a New and the Most Accessible Source of Mesenchymal Stem Cells from the Oral Cavity to Be Used in Regenerative Therapies. *Postepy Hig Med Dosw (Online)* **2016**, *70*, 858−871.

(32) Jia, W.; Li, M.; Liu, L.; Zhou, H.; Liu, X.; Gu, G.; Xiao, M.; Chen, Z. Fabrication and Assessment of Chondroitin Sulfate-Modified Collagen Nanofibers for Small-Diameter Vascular Tissue Engineering Applications. *Carbohydr. Polym.* **2021**, *257*, 117573.

(33) Rieu, C.; Parisi, C.; Mosser, G.; Haye, B.; Coradin, T.; Fernandes, F. M.; Trichet, L. Topotactic Fibrillogenesis of Freeze-Cast Micro-ridged Collagen Scaffolds for 3D Cell Culture. *ACS Appl. Mater. Interfaces* **2019**, *11*, 14672−14683.

(34) Rouhollahi, A.; Ilegbusi, O.; Florczyk, S.; Xu, K.; Foroosh, H. Effect of Mold Geometry on Pore Size in Freeze-Cast Chitosan-

Alginate Scaffolds for Tissue Engineering. *Ann Biomed Eng* **2020**, *48*, 1090−1102.
(35) Wu, J.; Zhao, Q.; Liang, C.; Xie, T. Enzymatically Degradable Oxidized Dextran−Chitosan Hydrogels with an Anisotropic Aligned Porous Structure. *Soft Matter* **2013**, *9*, 11136.
(36) Nagy, K.; Láng, O.; Láng, J.; Perczel-Kovách, K.; Gyulai-Gaál, S.; Kádár, K.; Kőhidai, L.; Varga, G. A Novel Hydrogel Scaffold for Periodontal Ligament Stem Cells. *Interv Med Appl Sci* **2018**, *10*, 1−9.
(37) Arpornmaeklong, P.; Sareethammanuwat, M.; Apinyauppatham, K.; Boonyuen, S. Characteristics and Biologic Effects of Thermosensitive Quercetin-Chitosan/Collagen Hydrogel on Human Periodontal Ligament Stem Cells. *J Biomed Mater Res B Appl Biomater* **2021**, *109*, 1656−1670.
(38) Pawitan, J. A. Prospect of Stem Cell Conditioned Medium in Regenerative Medicine. *Biomed Res Int* **2014**, *2014*, 1.
(39) Inukai, T.; Katagiri, W.; Yoshimi, R.; Osugi, M.; Kawai, T.; Hibi, H.; Ueda, M. Novel Application of Stem Cell-Derived Factors for Periodontal Regeneration. *Biochem. Biophys. Res. Commun.* **2013**, *430*, 763−768.
(40) Kyurkchiev, D.; Bochev, I.; Ivanova-Todorova, E.; Mourdjeva, M.; Oreshkova, T.; Belemezova, K.; Kyurkchiev, S. Secretion of Immunoregulatory Cytokines by Mesenchymal Stem Cells. *World J Stem Cells* **2014**, *6*, 552−570.
(41) Madrigal, M.; Rao, K. S.; Riordan, N. H. A Review of Therapeutic Effects of Mesenchymal Stem Cell Secretions and Induction of Secretory Modification by Different Culture Methods. *J Transl Med* **2014**, *12*, 260.
(42) Li, H.; Cheng, F.; Wei, X.; Yi, X.; Tang, S.; Wang, Z.; Zhang, Y. S.; He, J.; Huang, Y. Injectable, Self-Healing, Antibacterial, and Hemostatic N,O-Carboxymethyl Chitosan/Oxidized Chondroitin Sulfate Composite Hydrogel for Wound Dressing. *Materials Science and Engineering: C* **2021**, *118*, 111324.
(43) Shin, J.; Kang, E. H.; Choi, S.; Jeon, E. J.; Cho, J. H.; Kang, D.; Lee, H.; Yun, I. S.; Cho, S.-W. Tissue-Adhesive Chondroitin Sulfate Hydrogel for Cartilage Reconstruction. *ACS Biomater Sci Eng* **2021**, *7*, 4230−4243.
(44) Das, P.; Salerno, S.; Remigy, J.-C.; Lahitte, J.-F.; Bacchin, P.; De Bartolo, L. Double porous poly (??-caprolactone)/chitosan membrane scaffolds as niches for human mesenchymal stem cells. *Colloids Surf B Biointerfaces* **2019**, *184*, 110493.
(45) Perez, R. A.; Mestres, G. Role of Pore Size and Morphology in Musculo-Skeletal Tissue Regeneration. *Mater Sci Eng C Mater Biol Appl* **2016**, *61*, 922−939.
(46) Zhang, Q.; Shi, S.; Liu, Y.; Uyanne, J.; Shi, Y.; Shi, S.; Le, A. D. Mesenchymal Stem Cells Derived from Human Gingiva Are Capable of Immunomodulatory Functions and Ameliorate Inflammation-Related Tissue Destruction in Experimental Colitis. *J. Immunol.* **2009**, *183*, 7787−7798.
(47) Lu, Y.; Xu, Y.; Zhang, S.; Gao, J.; Gan, X.; Zheng, J.; Lu, L.; Zeng, W.; Gu, J. Human Gingiva-Derived Mesenchymal Stem Cells Alleviate Inflammatory Bowel Disease via IL-10 Signalling-Dependent Modulation of Immune Cells. *Scand. J. Immunol.* **2019**, *90*, No. e12751.
(48) Watanabe, Y.; Fukuda, T.; Hayashi, C.; Nakao, Y.; Toyoda, M.; Kawakami, K.; Shinjo, T.; Iwashita, M.; Yamato, H.; Yotsumoto, K.; Taketomi, T.; Uchiumi, T.; Sanui, T.; Nishimura, F. Extracellular Vesicles Derived from GMSCs Stimulated with TNF-α and IFN-α Promote M2 Macrophage Polarization via Enhanced CD73 and CD5L Expression. *Sci. Rep.* **2022**, *12*, 13344.
(49) Tavelli, L.; McGuire, M. K.; Zucchelli, G.; Rasperini, G.; Feinberg, S. E.; Wang, H.-L.; Giannobile, W. V. Extracellular Matrix-Based Scaffolding Technologies for Periodontal and Peri-Implant Soft Tissue Regeneration. *J Periodontol* **2020**, *91*, 17−25.

https://doi.org/10.1021/acsbiomaterials.2c01440
ACS Biomater. Sci. Eng. XXXX, XXX, XXX−XXX